December 2008 Volume 3 Issue 2-3

Trade Science Inc.

Physical CHEMISTRY
An Indian Journal

Full Paper

PCAIJ, 3(2-3), 2008 [81-86]

Characterization and thermoelectric properties of $Na_xCo_2O_4$ by the polymerized complex method

Weerasak Somkhunthot*,Thanusit Burinprakhon, Nuwat Pimpabute,Tosawat Seetawan, Anek Charoenphakdee, Vittaya Amornktibamrung

Physics Department, Faculty of Science, Khon Kaen University, 123 Mittapap Road, Muang District, Khon Kaen 40002, (THAILAND)

Received: 28th July, 2008 ; Accepted: 2nd August, 2008

ABSTRACT

The thermoelectric oxide $Na_xCo_2O_4$ was synthesized by the polymerized complex method and was characterized by XRD, TEM, FE-SEM, and EDS. It was found that the calcined powder showed a γ-$Na_xCo_2O_4$ phase without any impurity phase while the sintered pellet detected the Na_2CO_3, Na_2O, and Co_3O_4 phases. However, these products are the polycrystalline hexagonal, the same average particle size and morphology of the layer structure, several samples are agglomerated and each particle is flaky, and the sodium contents of the samples are more than 1.5. Moreover, the thermoelectric properties show the high Seebeck coefficient, the low electrical resistivity, and the large power factor.

KEYWORDS

Characterization of $Na_xCo_2O_4$;
Thermoelectric oxide $Na_xCo_2O_4$;
Polymerized complex method.

1. INTRODUCTION

Up to now, fossil fuels have been the main energy resources of the world. More than 80% of its primary energy needs has been supplied by petroleum oil, natural gas, and coal. However, these energy resources are non-renewable and cause problems to the environment as a result of their relatively high amount of carbon dioxide (CO_2), carbon monoxide (CO), and other environmentally harmful emissions. This has been a driving force to look for alternative energy resources which are clean, safe, and long-term reliable. Thermoelectricity is one of the renewable energy resources that has been widely investigated and is expected to be feasible in the near future. Despite giving low efficiency in energy conversion, thermoelectric technology holds promise for clean energy generation, since it can directly convert heat to electrical energy by using non-polluting thermoelectric devices. The technology is very suitable for hot countries like Thailand where heat from the sun is available throughout the year. Thermoelectric devices operate based on the thermoelectric phenomena occurring in thermoelectric materials subjected to a temperature gradient and, hence, contain no moving parts and are highly reliable. These are reasons for the growing interest in further research and development of the technology.

The performance of a thermoelectric device is determined by the dimensionless figure of merit ZT given by $ZT = S^2T/\rho\kappa$. The thermoelectric parameters S, ρ, κ are the Seebeck coefficient, the electrical resistivity, and the thermal conductivity of the thermoelectric materials

Full Paper

used to fabricate the device, respectively. T is the absolute temperature in K at which the device operates. Higher ZT values lead to thermoelectric devices of improved performance. In other words, good thermoelectric materials, which are defined as materials of high S, low ρ, and low κ, are crucial for the fabrication of high efficiency thermoelectric devices. The thermoelectric parameters S, ρ, κ, and, hence, ZT are dependent on materials and their properties. The highest ZT of about 1.0 has been achieved from the state of the art thermoelectric material Bi_2Te_3, at room temperature[1,2]. Both theoretical and experimental approaches have been conducted to search for new materials of higher ZT. This has been the important task in the development of thermoelectric technology.

Among those materials investigated, a transition metal oxide $Na_xCo_2O_4$ has been expected to be one of the candidates for good thermoelectric materials. This new thermoelectric material has been reported to exhibit a large thermoelectric power with a low resistivity[3]. Its room temperature ZT value is comparable to that of Bi_2Te_3[4]. This finding has triggered intensive studies on the thermoelectric properties of the material. Within the past few years, there have been a number of papers reporting the preparation of powder and bulk $Na_xCo_2O_4$ by several methods including the conventional solid state reaction (SSR) method and the polymerized complex (PC) method or citric acid complex (CAC) method. It has been found that the thermoelectric properties of $Na_xCo_2O_4$ are dependent on the preparation method and types of metal added[5]. The Seebeck coefficient of PC or CAC samples is significantly higher than that of SSR samples. The maximum ZT value of 0.8 was obtained for the PC sample at 955 K, which is higher than ZT value of 0.5 for the SSR sample[6,7]. The improvement in ZT is believed to be due to the finer crystalline grain sizes of the sample prepared through the PC route. Doping with metals such as Ag shows strong influence on the thermoelectric properties of $Na_xCo_2O_4$. For example, the ZT of an Ag-doped sample was found to be higher than that of the non-doped sample, and reached ZT of 0.12 at 973 K[8-10]. The roles of the added metals in the ZT modification are still unclear[11].

In this study, we have investigated the samples characterization and the thermoelectric properties of the $Na_xCo_2O_4$ compound which was synthesized by the polymerized complex method.

2. EXPERIMENTAL

Polycrystalline samples of $Na_xCo_2O_4$ were synthesized from a powder precursor prepared by the Polymerized Complex (PC) process. In the PC method, citric acid ($C_6H_8O_7.H_2O$ 210.14 g/mol, 99.7% purity, AnalaR®, VWR International Ltd., England) was firstly dissolved in ethylene glycol ($HOCH_2CH_2OH$ 62.07 g/mol, 99.5% purity, AnalaR®, VWR International Ltd., England). Subsequently, cobalt (II) nitrate ($Co(NO_3)_2.6H_2O$ 291.03 g/mol, 98-102.0% purity, UNIVAR, APS Chemicals Limited, Australia) and sodium nitrate ($NaNO_3$ 84.99 g/mol, 99.5% purity, AnalaR®, VWR International Ltd., England) in a molar ratio were added to this solution. The mixture solution was then stirred and heated at 573 K. During this heating process, the formation of the polymer between ethylene glycol and metal citrate complexes occurred. As the colloidal solution was condensed, it became a highly viscous polymeric product which was then decomposed to a dark mass precursor at 723 K for 1 h in air. This dark mass precursor was ground and calcined at 1073 K for 5 h in order to obtain the γ-$Na_xCo_2O_4$ phase. The calcined powder precursor was compacted under a pressure of 150 MPa into pellets of 60 mm diameter and 2.5 mm thick. The pellet precursor was then subjected to a sintering process at 1173 K for 24 h in air. Since Na tends to evaporate during the heating processes, excessive amounts of Na (20% extra) were initially applied in the PC process in order to obtain the nominal composition of the sintered pellet to be $Na_xCo_2O_4$ with $x > 1.5$. The synthesis of the polycrystalline samples of $Na_xCo_2O_4$ thermoelectric oxides by the PC method was summarized in figure 1.

Phase identification of the $Na_xCo_2O_4$ Compounds (decomposed dark mass, calcined powder, and sintered pellet) was examined by X-ray diffraction (XRD, PW3043 Philips X-ray diffractometer of The Netherlands) at room temperature using CuKα radiation, λ = 0.15406 nm. Each sample was measured in the data angle range of $10^o \le 2\theta \le 70^o$ with scanning rate 0.04 2θ/sec. The lattice parameter of the samples was calculated from the XRD patterns. The crystal structures were analyzed using the transmission electron microscopy

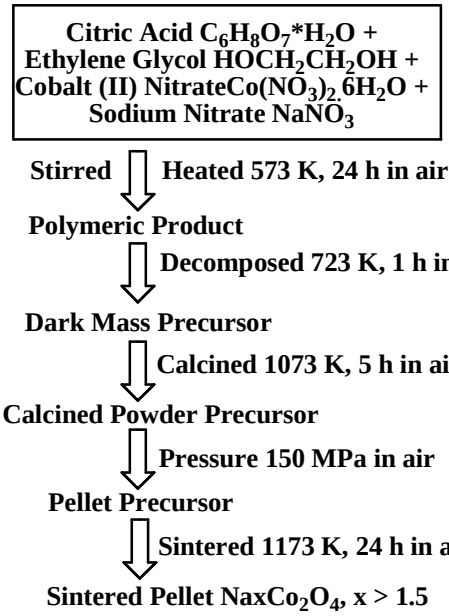

Figure 1: Fabrication flow chart for the polymerized complex procedure used to prepare the polycrystalline samples of the $Na_xCo_2O_4$ thermoelectric oxides

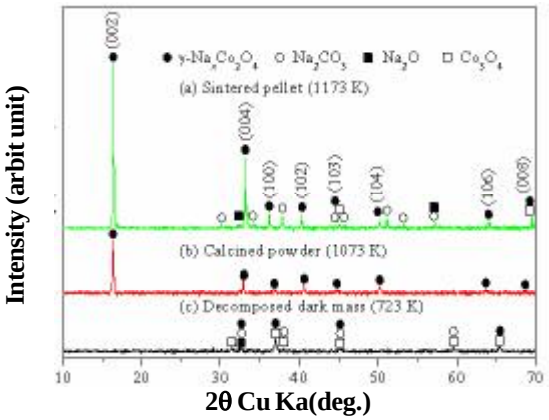

Figure 2: XRD patterns of the γ-$Na_xCo_2O_4$ compounds

TABLE 1 : Characteristics of the γ-$Na_xCo_2O_4$ compounds

Sample	Lattice parameter		Absolute error
	a (nm)	c (nm)	(%)
Decomposed dark mass (723 K)	0.28932	1.13597	±0.00247
Calcined powder (1073 K)	0.28274	1.09448	±0.00033
Sintered pellet (1173 K)	0.28405	1.07909	±0.00016

(TEM, JEM-2010, Japan). Observations on the fracture surfaces were carried out using a field emission scanning electron microscope (FE-SEM, JSM-6335F, Japan) and energy dispersive spectroscopy (EDS, JSM-6335F, Japan).

Density (d) of the sample was determined from the measured weight and dimensions. The thermoelectric properties were measured in the temperature range of 300–803 K. The Seebeck coefficient (S) and electrical resistivity (ρ) were measured by ULVAC ZEM-1 in helium atmosphere with dimensions of 3.0mm × 3.0mm × 20mm. The temperature gradients were about 20, 30, and 40 K.

3. RESULTS AND DISCUSSION

3.1 Samples characterization

The XRD patterns of the γ-$Na_xCo_2O_4$ compounds were acquired on a Philips X'Pert Plus as shown in figure 2. The intensity of (002) and (004) of peaks of the sintered pellet and calcined powder were relatively large compared to the other peak. The small peaks of the Na_2CO_3, Na_2O, and Co_3O_4 phases were detected in the pattern of the pellet sample, while the powder sample was composed of the γ-$Na_xCo_2O_4$ phase without any impurity phase. The resulting XRD patters were likely to report by Ito et al.[6]. The precipitation of these Co_3O_4 is considered to be due to Na evaporation during the sintering. For the decomposed dark mass precursor is not the completely crystal. The degree of crystallographic orientation of these samples was evaluated using the Lotgering factor[12], $f = (P-P_0)/(1-P_0)$, where $P = \Sigma I(00l)/\Sigma I(hkl)$, and $P_0 = P$ for a crystallographically isotropic sample. The P_0 was calculated from the peak data on the JCPDS card, no. 73-0133. The c-axis directions are completely aligned when f = 1. The sintered sample showed the highest degree of orientation and has a comparatively large f value, 0.89. The characteristics of the $Na_xCo_2O_4$ compounds are shown in TABLE 1. The hexagonal lattice parameters a and c determined from the XRD patterns of the γ-$Na_xCo_2O_4$ phase. The results show that the lattice parameters were similar to data reported by Seetawan et al.[11]. However, the lattice parameter c of the sintered pellet is less than calcined powder, about 0.01539 nm, while the decomposed dark mass is greater than calcined powder, about 0.04149 nm. The Sherrer calculator determine that the decomposed dark mass and the calcined powder have crystallite size and lattice strain 38.7250±10.1656 nm, 0.2545% and 38.5143± 22.3132 nm, 0.1447%, respectively.

The TEM images and corresponding selected area

Full Paper

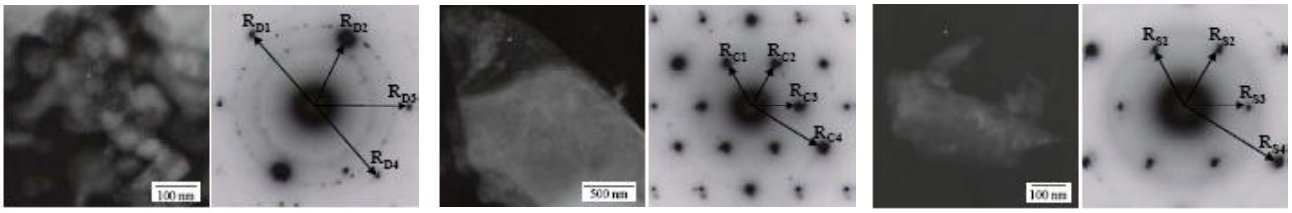

(a) Decomposed dark mass (723 K), L = 80 cm, λ = 0.0253Å, Lλ = 20.2530 mm·Å

(b) Calcined powder (1073 K), L = 60 cm, λ = 0.0259Å, Lλ = 15.5430 mm·Å

(c) Sintered pellet (1173), L = 80 cm, λ = 0.0253Å, Lλ = 20.2530 mm·Å

Figure 3 : TEM images and SAED patterns of the γ-$Na_xCo_2O_4$ compounds

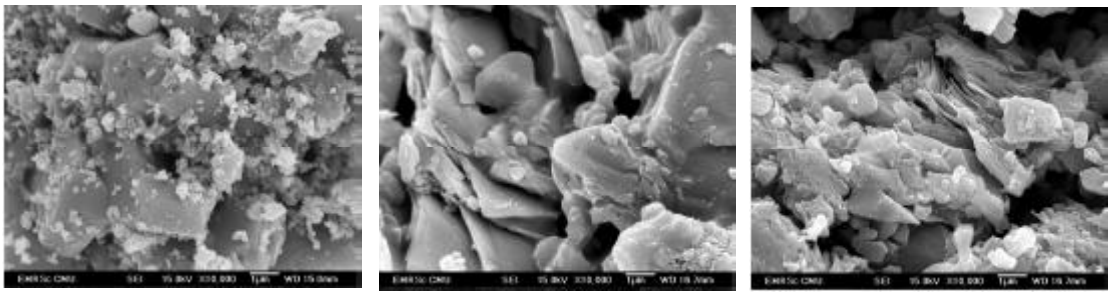

Figure 4 : FE-SEM micrographs of the γ-$Na_xCo_2O_4$ compounds

TABLE 2: Vector, d-spacing, and Miller index (hkl) of the γ-$Na_xCo_2O_4$ compounds

Sample	Vector	d-spacing (Å)	(hkl)
Decomposed dark mass (723 K) L = 80 cm, λ = 0.0253Å, Lλ = 20.2530 mm·Å	R_{D1}	1.6510	-
	R_{D2}	2.1559	-
	R_{D3}	1.6878	-
	R_{D4}	1.6819	-
Calcined powder (1073 K) L = 60 cm, λ = 0.0259Å, Lλ = 15.5430 mm·Å	R_{C1}	2.4619	(100)
	R_{C2}	2.4619	(100)
	R_{C3}	2.4671	(100)
	R_{C4}	1.4249	(110)
Sintered pellet (1173 K) L = 80 cm, λ = 0.0253Å, Lλ = 20.2530 mm·Å	R_{S1}	2.4609	(100)
	R_{S2}	2.4609	(100)
	R_{S3}	2.4699	(100)
	R_{S4}	1.4245	(110)

TABLE 3 : Relationship between atomic weight (%) for the γ-$Na_xCo_2O_4$ compounds

Element/Sample	Atomic weight (%)			$Na_xCo_2O_4$
	Na	Co	O	
Decomposed dark mass (723 K)	26.68	30.53	42.79	$Na_{1.73}Co_2O_4$
Calcined powder (1073 K)	20.58	48.93	30.48	$Na_{1.88}Co_2O_4$
Sintered pellet (1173 K)	20.57	49.10	30.33	$Na_{1.89}Co_2O_4$

electron diffraction (SAED) patterns of the γ-$Na_xCo_2O_4$ samples are shown in figure 3. The results show the spot patterns which can be calculated the d-spacing and indexed Miller index (hkl) as shown in TABLE 2. These respondents indicated that the calcined and sintered samples are the polycrystalline hexagonal structure which was close to the standard indexed diffraction pattern for hcp crystal[13]. Thus, TEM results suggested and confirmed that the $Na_xCo_2O_4$ products are the polycrystalline hexagonal.

The FE-SEM micrographs of the γ-$Na_xCo_2O_4$ samples are shown in figure 4 at magnification of ×10000. From this figure, the calcined powder and sintered pellet exhibited the same average particle size and the same morphology of the layer structure, several samples are agglomerated and each particle is flaky. These results were the same as the micrographs of Masuda et al.[14].

The EDS analysis revealed that the atomic weights (%) of Na, Co and O for the $Na_xCo_2O_4$ samples as shown in figure 5 and TABLE 3. The sodium content of decomposed dark mass, calcined powder and sintered pellet samples were about 1.73, 1.88 and 1.89, respectively. The nominal compositions of the samples indicated that the preparations of $Na_xCo_2O_4$ compounds have been successfully synthesized by the polymerized complex (PC) route.

3.2 Thermoelectric properties

The electrical resistivity, ρ, and Seebeck coefficient, S, of the sintered sample was measured using the range temperature from room temperature to 803 K. Figures 6 and 7 show the low ρ and high S. At 803 K, these values are equal to 18.8 μΩ·m and 178 μV/K, respectively. This sample showed that the good thermoelectric material.

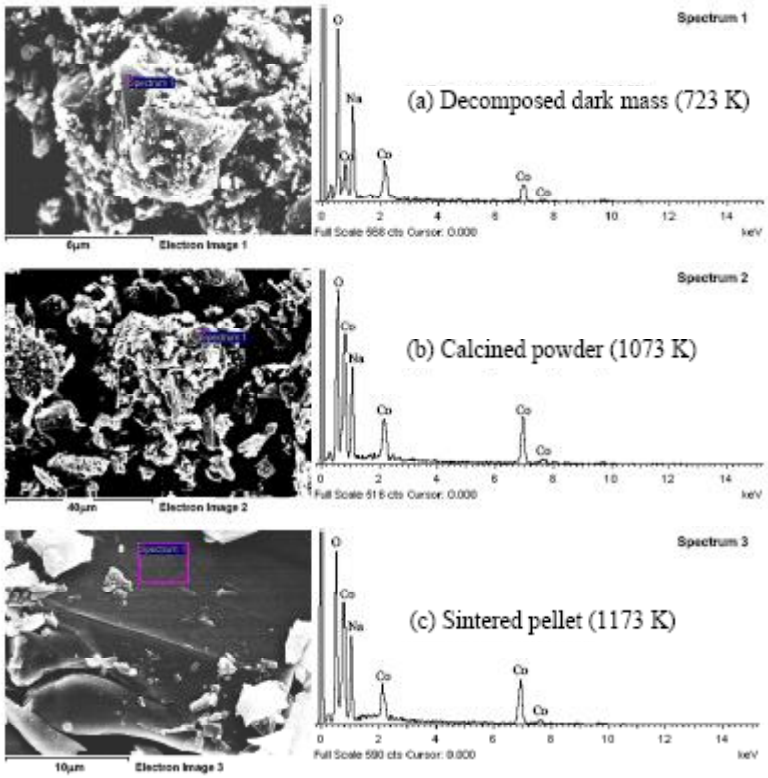

Figure 5 : EDS images and spectrums of the γ-$Na_xCo_2O_4$ microstructures

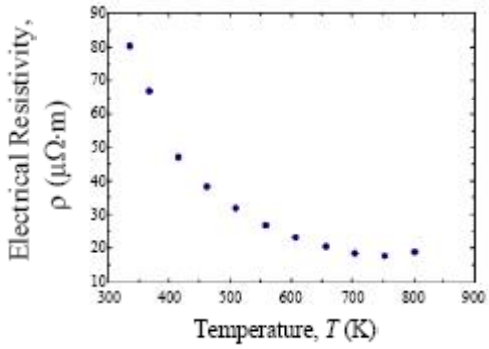

Figure 6 : Electrical resistivity of the γ-$Na_xCo_2O_4$ as a function of temperature

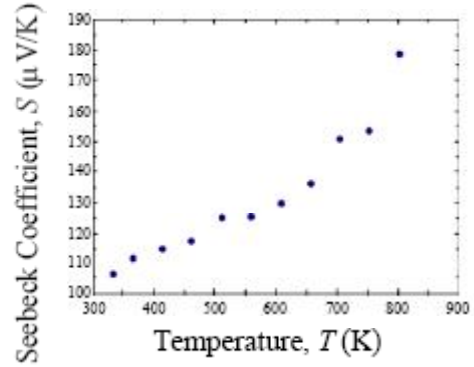

Figure 7 : Seebeck coefficient of the γ-$Na_xCo_2O_4$ as a function of temperature

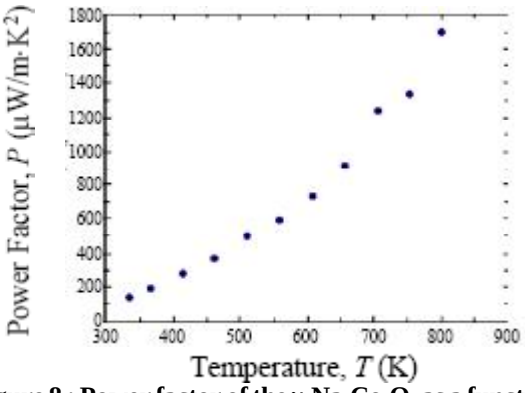

Figure 8 : Power factor of the γ-$Na_xCo_2O_4$ as a function of temperature

The power factor, P, of this samples was calculated from the S and the ρ in the equation $P = S^2/\rho$. Figure 8 shows the temperature dependence of the power factor and the large P values were attributable to the large Seebeck coefficient which was similar to the procedure reported by Ito et al.[7].

3. CONCLUSIONS

The thermoelectric oxide $Na_xCo_2O_4$ was synthesized by the polymerized complex method and was characterized. The XRD identified that the calcined

Full Paper

powder showed a γ-$Na_xCo_2O_4$ phase without any impurity phase while the sintered pellet detected the Na_2CO_3, Na_2O, and Co_3O_4 phases. The TEM results suggested and confirmed that the γ-$Na_xCo_2O_4$ products are the polycrystalline hexagonal. The FE-SEM micrographs showed that the calcined powder and sintered pellet exhibited the same average particle size and the same morphology of the layer structure, several samples are agglomerated and each particle is flaky. The EDS analyzed that the sodium content of powder and pellet samples are more than 1.5. The thermoelectric properties show the low electrical resistivity, 18.8 μΩ·m, and high Seebeck coefficient, 178 μV/K, at 803 K. The power factor shows the temperature dependence of the power factor and the large P values were attributable to the large Seebeck coefficient. The resulting indicated that the preparation of $Na_xCo_2O_4$ compounds has been successfully synthesized.

ACKNOWLEDGMENTS

This work was financially supported by the Commission on Higher Education (Ministry of Education), Physics Department, Faculty of Science, Khon Kaen University and Loei Rajabhat University. We thank Ken Kurosaki and Shinsuke Yamanaka (Osaka University) for thermoelectric characterizations our thanks to Ian Thomas for editing the manuscript..

REFERENCES

[1] L.M.Goncalves, C.Couto, P.Alpuim, D.M.Rowe, J.H.Correia; The 13th International Conference on Solid-State Sensors, Actuators and Microsystems Seoul, Korea: IEEE, 904-907 **(2005)**..

[2] H.Wang, W.D.Porter, J.Sharp; International Conference on Thermoelectrics, Dallas, Texas: IEEE, 91-94 **(2005)**.

[3] M.Jansen, R.Hoppe; Zeitschrift für Anorganische und Allgemeine Chemie, **408(2)**, 104-106 **(1974)**.

[4] I.Terasaki, Y.Sasago, K.Uchinokura; Physical Review B, **56(20)**, R12 685-R12 687 **(1997)**.

[5] T.Nagira, M.Ito, S.Katsuyama, M.Mjima, H.Nagai; Journal of Alloys and Compounds, **348(1-2)**, 263-269 **(2003)**.

[6] M.Ito, T.Nagira, D.Furumoto, S.Katsuyama, H. Nagai; Scripta Materialia, **48(4)**, 403-408 **(2003)**.

[7] M.Ito, T.Nagira, D.Furumoto, Y.Oda, S.Hara; Science and Technology of Advanced Materials, **5(1-2)**, 125-131 **(2004)**.

[8] T.Seetawan, V.Amornkitbamrung, T.Burinprakhon, S.Maensiri, K.Kurosaki, H.Muta, M.Uno, S.Yamanaka; Journal of Alloys and Compounds, **403(1-2)**, 308-311 **(2005)**.

[9] T.Seetawan, V.Amornkitbamrung, T.Burinprakhon, S.Maensiri, K.Kurosaki, H.Muta, M.Uno, S.Yamanaka; Journal of Alloys and Compounds, **407(1-2)**, 314-317 **(2006)**.

[10] T.Seetawan, V.Amornkitbamrung, T.Burinprakhon, S.Maensiri, K.Kurosaki, H.Muta, M.Uno, S. Yamanaka; Journal of Alloys and Compounds, **414(1-2)**, 293-297 **(2006)**.

[11] T.Seetawan, V.Amornkitbamrung, T.Burinprakhon, S.Maensiri, P.Tongbi, K.Kurosaki, H.Muta, M.Uno, S.Yamanaka; Journal of Alloys and Compounds, **416(1-2)**, 291-295 **(2006)**.

[12] F.K.Lotgering; Journal of Inorganic and Nuclear Chemistry, **9(2)**, 113-123 **(1975)**.

[13] D.B.Williams, C.B.Cartar; 'Transmission Electron Microscopy', New York: Plenum Press, **(1996)**.

[14] Y.Masuda, Y.Hamada, W.S.Seo, K.Koumoto; Journal of Nanoscience and Nanotechnology, **6**, 1632-1638 **(2006)**.